



Published in final edited form as:

Gut. 2023 October ; 72(10): 1942–1958. doi:10.1136/gutjnl-2022-327924.

MicroRNA-223 attenuates hepatocarcinogenesis by blocking hypoxia-driven angiogenesis and immunosuppression

Yaojie Fu¹, Bryan Mackowiak¹, Dechun Feng¹, Hongkun Lu¹, Yukun Guan¹, Taylor Lehner¹, Hongna Pan¹, Xinwei Wang^{2,3}, Yong He^{1,*}, Bin Gao^{1,*}

¹Laboratory of Liver Diseases, National Institute on Alcohol Abuse and Alcoholism, National Institutes of Health, Bethesda, MD, USA

²Laboratory of Human Carcinogenesis, Center for Cancer Research, National Cancer Institute, National Institutes of Health, Bethesda, MD, USA

³Liver Cancer Program, Center for Cancer Research, National Cancer Institute, National Institutes of Health, Bethesda, MD, USA.

Abstract

Objective: The current treatment for hepatocellular carcinoma (HCC) to block angiogenesis and immunosuppression provides some benefits only for a subset of HCC patients, thus optimized therapeutic regimens are unmet needs, which require a thorough understanding of the underlying mechanisms by which tumor cells orchestrate an inflamed tumor microenvironment with significant myeloid cell infiltration. MicroRNA-223 (miR-223) is highly expressed in myeloid cells but its role in regulating tumor microenvironment remains unknown.

Design: Wild-type and miR-223 knockout mice were subjected to two mouse models of inflammation-associated HCC induced by injection of diethylnitrosamine (DEN) or orthotopic HCC cell implantation in chronic carbon tetrachloride (CCl₄)-treated mice.

Results: Genetic deletion of miR-223 markedly exacerbated tumorigenesis in inflammation-associated HCC. Compared to wild-type mice, miR-223 knockout mice had more infiltrated programmed cell death 1 (PD-1⁺) T cells and programmed cell death ligand 1 (PD-L1⁺) macrophages after DEN+CCl₄ administration. Bioinformatic analyses of RNA-Seq data revealed a strong correlation between miR-223 levels and tumor hypoxia, a condition that is well-documented to regulate PD-1/PD-L1. *In vivo* and *in vitro* mechanistic studies demonstrated that miR-223 did not directly target PD-1 and PD-L1 in immune cells rather than indirectly downregulated them by modulating tumor microenvironment via the suppression of hypoxia-inducible factor 1 α (HIF-1 α)-driven CD39/CD73-adenosine pathway in HCC. Moreover, gene delivery of miR-223 via adenovirus inhibited angiogenesis and hypoxia-mediated PD-1/PD-L1 activation in both HCC models, thereby hindering HCC progression.

*Corresponding authors: Bin Gao, M.D., Ph.D., Laboratory of Liver Diseases, NIAAA/NIH, 5625 Fishers Lane, Bethesda, MD 20892; bgao@mail.nih.gov; or Yong He, Ph.D., Laboratory of Liver Diseases, NIAAA/NIH, 5625 Fishers Lane, Bethesda, MD 20892; heyong@simm.ac.cn.
Current address: Yong He, Ph.D., Shanghai Institute of Materia Medica (SIMM), Chinese Academy of Sciences, Shanghai, China.

Conclusion: miR-223 plays a critical role in modulating hypoxia-induced tumor immunosuppression and angiogenesis, which may serve as a novel therapeutic target for HCC.

Introduction

Tumor microenvironment, which is characterized by enhanced angiogenesis and immunosuppression, plays a critical role in promoting tumor development and is closely associated with a poor survival rate.¹ Targeting microenvironment via the combination therapy of anti-angiogenic agents and immune checkpoint inhibitors has shown some clinical benefits only in a subset of patients with hepatocellular carcinoma (HCC).² Thus, optimized therapeutic regimens for most HCC patients are still urgently needed. To develop such therapies, we need to better understand HCC tumor microenvironment. The majority of HCC develops post chronic liver injury and inflammation from different etiologies, including viral hepatitis, alcohol-associated liver disease and nonalcoholic fatty liver disease.^{3, 4} Chronic liver inflammation is strongly associated with intrahepatic infiltration of myeloid cells such as macrophages and neutrophils,³⁻⁸ however, how myeloid cells regulate tumor microenvironment and HCC progression is still poorly understood.

MicroRNA-223 (miR-223) is a well-documented myeloid-enriched miRNA that acts as an important anti-inflammatory regulator, thereby preventing liver disease progression.⁹ MiR-223 is expressed at the highest levels in neutrophils, followed by macrophages, but it is expressed at low levels in hepatocytes.¹⁰ It has been reported that miR-223 inhibits liver inflammation by attenuating the NLRP3 inflammasome,^{11, 12} the NF- κ B pathway,¹³ CXCL10,¹⁴ etc. Given myeloid cells are enriched in human HCC,³⁻⁸ we speculate that myeloid-enriched miR-223 may play a critical role in regulating tumor microenvironment and modulating HCC progression, but its exact role remains unknown. MiR-223 levels were reported to be significantly decreased in HCC tissues¹⁵ and in the plasma from HCC patients.¹⁶ Additionally, miR-223 has been verified as a prognostic indicator for HCC patients^{17, 18} Mechanistic studies suggest that miR-223 downregulates the expression of stathmin 1, a multifunctional oncogene, to repress HCC.¹⁵ Although the downregulation of miR-223 is well documented in HCC, little is known about the roles of miR-223 in modulating tumor angiogenesis, immune response and HCC therapy.

In the current study, we examined the functions of miR-223 in modulating HCC tumor microenvironment by using two mouse HCC models with chronic liver inflammation, including injection of diethylnitrosamine (DEN) plus chronic carbon tetrachloride (CCl₄) injection,¹⁹ and implantation of HCC cells plus chronic CCl₄ injection. Our data suggest that miR-223 targets hypoxia inducible factor 1 α (HIF-1 α) in HCC and subsequently suppresses immune checkpoint PD1/PD-L1 expression by downregulating the hypoxia-driven CD39 (ecto-nucleoside triphosphate diphosphohydrolase 1, E-NTPDase1)/ CD73 (ecto-5'-nucleotidase, Ecto5'NTase)-adenosine pathway,²⁰⁻²³ thereby inhibiting HCC. Finally, we demonstrated that gene delivery of miR-223 inhibited tumor growth, hypoxia, angiogenesis and immunosuppression in two preclinical models of HCC, implying miR-223 serves as a novel therapeutic target for HCC therapy.

Methods and Materials

Mice

MiR-223 knockout (miR-223KO) and male C57B/6J mice were purchased from The Jackson Laboratory (Bar Harbor, ME). Male miR-223^{-y} (KO, the miR-223 locus is on the X chromosome) and littermate miR-223^{+y} (wild-type, WT) mice were obtained via the breeding of male miR-223^{-y} and female miR-223^{+/-} mice. Mouse experiments were approved by the NIAAA Animal Care and Use Committee.

DEN+CCl₄ induced HCC mouse model

Male miR-223KO and littermate WT mice were administered with a single dose of N-nitrosodiethylamine (DEN) (Sigma-Aldrich, St. Louis, MO) (i.p. injection of 25 mg/kg at 15 days of age), followed by chronic carbon tetrachloride (CCl₄) (Sigma-Aldrich) treatment (starting at 8 weeks of age; 2 ml/kg, 10% dissolved in olive oil, once per week via i.p. injection) for continuous 21 weeks, to induce HCC model as described previously.¹⁹ Mice were also subjected to single DEN injection or chronic CCl₄ alone.²⁴

Inflammation associated hepatoma cell implanted HCC model

Twelve- to fourteen-week-old male miR-223KO, WT, and C57BL6/J mice were treated with chronic CCl₄ for 2 weeks. Murine hepatoma Hepa1-6 cells (ATCC CRL-1830) were resuspended (3.0×10^5 cells in 20 μ L phosphate-buffered saline per mouse) and mixed with 20 μ L Matrigel Matrix Basement Membrane High Concentration (per mouse) (Corning, Inc., Corning, NY). The cell mixture was orthotopically implanted at the margin of major lobes in mouse livers, and the implanted mice were treated with chronic CCl₄ for 2 more weeks.

Statistical analysis

Data are presented as the means \pm SEM and were analyzed by using GraphPad Prism software (v. 7.0; GraphPad Software, La Jolla, CA). To compare values from 2 groups, significance was evaluated by Student's *t*-test. Data from multiple groups were compared with one-way ANOVA followed by Tukey's post hoc test. Pearson correlation analysis was performed to evaluate linear relationship of two parameters. All statistical tests were two-sided. *P* values of < 0.05 were considered to be statistically significant.

All other methods are included in the Supporting materials.

Results

MiR-223 attenuates tumor development and angiogenesis in DEN+CCl₄-induced inflammation-associated HCC

To address the role of miR-223 in HCC development, we used several models including single DEN injection, DEN+CCl₄ injection, and chronic CCl₄ injection. Our data revealed that miR-223 KO mice developed less HCC in the single DEN model (Supporting Fig. S1A–C) but more HCC in the DEN+CCl₄ model (Fig. 1A) compared to their corresponding WT controls. Chronic CCl₄ injection did not induce HCC in WT or miR-223 KO mice (data not shown). Our data suggest that miR-223 directly promotes a single dose of DEN-

induced HCC that has little inflammation but suppresses inflammation-associated HCC in the DEN+CCl₄ model. Because the DEN+CCl₄ model is more relevant to human HCCs that are associated with strong inflammation,¹⁹ we focused on this DEN+CCl₄ model in the current study.

Compared to WT mice, miR-223KO mice had greater tumor masses and number of DEN+CCl₄ HCC, and more progressively proliferative capacity than WT mice as demonstrated by higher mRNA levels of HCC biomarkers (*Afp*, *Gpc3*, *Golm1* and *Tff3*) and Ki67 index (a marker for tumor proliferation) (Fig. 1A–D). Interestingly, as a hallmark of tumor growth, angiogenesis of HCC tumor region (T) in miR-223KO mice was greater than that in WT mice, which was evidenced by higher CD31 (a marker for endothelial cell) expression, elevated expression of angiogenesis related genes (*Endoglin*, *Vegf*) and phosphorylated vascular endothelial growth factor receptor 2 (VEGFR2) protein (Fig. 1C–F). Next, we examined miR-223 levels and found that miR-223 expression was remarkably elevated in both HCC tumor and adjacent non-tumor tissues compared to healthy control livers with lower levels in tumor tissues than in adjacent non-tumor tissues (Supporting Fig. S1D). Analyses of TCGA database revealed that similar downregulation of miR-223 expression was also observed in human HCC tissues vs non-tumor liver tissues (Supporting Fig. S1E).

MiR-223 attenuates chronic inflammation and PD-1/PD-L1 activation in DEN+CCl₄-induced HCC

To compare the inflammatory tumor microenvironment between WT and miR-223KO mice in the DEN+CCl₄ model, we performed several experiments. First, H&E and immunohistochemistry detected a large number of infiltrating immune cells in tumor-adjacent regions with a greater number of neutrophil (MPO⁺) and macrophage (F4/80⁺) infiltration in the livers from miR-223KO mice compared to those from WT mice (Fig. 2A–B). Additionally, greater liver inflammation and fibrosis were observed in miR-223KO mice than that in WT mice (Supporting Fig. S1F, Supporting Fig. S2A–B). Second, we examined the expression of several well-defined immune checkpoint molecules in both tumor and adjacent non-tumor tissues. Compared to WT mice, miR-223KO mice had higher expression of 3 genes including *Pdcd1* (encodes PD-1), *Cd274* (encodes PD-L1), and *Cd272* (also known as *Btla*) in adjacent non-tumor tissues (Fig. 2C, Supporting Fig. S2C), while the expression of these genes in tumor tissues was comparable between these two groups (Fig. 2C). Next, we further characterized expression of PD-1 and PD-L1 in normal control livers (set as control), tumor and adjacent non-tumor samples from WT and miR-223KO mice. As illustrated in Fig. 2D, both proteins were detected at very low levels in normal livers but were upregulated in tumor and adjacent nontumor tissues. Expression levels of both proteins from adjacent nontumor tissues were higher in miR-223KO mice than those in WT mice, while expression of those proteins in tumor tissues was comparable between these two groups (Fig. 2D). Importantly, *Pdcd1* or *Cd274* mRNA levels in adjacent nontumor samples positively correlated with tumor numbers in DEN+CCl₄ model (Fig. 2E). Intriguingly, such PD-1 and PD-L1 elevations in miR-223KO mice observed in the DEN+CCl₄ model were not observed in chronic CCl₄ alone or single DEN-induced HCC model (Supporting Fig.

S2D–F), suggesting that PD-1/PD-L1 induction depends on the synergistic effect of chronic inflammation and tumor cells.

MiR-223 inhibits PD-1⁺ T cells and PD-L1⁺ macrophages in DEN+CCl₄ -induced HCC

Next, we sought to identify the PD-1⁺ and PD-L1⁺ cell types by performing flow cytometric and immunohistochemistry analyses. As illustrated in Fig. 3A–B, Supporting Fig. S3A, flow cytometric analysis revealed that PD-1 expression was detected in both CD4⁺ and CD8⁺ T cells, while PD-L1 was mainly detected in infiltrating CCR2⁺CD11b⁺ macrophages from DEN+CCl₄-treated WT mice. Double immunostaining confirmed that most of PD-L1⁺ cells were IBA⁺ macrophages (Supporting Fig. S3B). Finally, immunostaining revealed that the number of PD-1⁺ and PD-L1⁺ cells were much greater in the livers of miR-223KO mice compared with WT mice after DEN+CCl₄ challenge (Fig. 3C–D, Supporting Fig. S3C).

Hif-1a is a target of MiR-223 in HCC

Next, we explored the underlying mechanism by which miR-223 regulates PD-1/PD-L1 expression. To test whether miR-223 directly regulates PD-1/PD-L1, we transfected mouse macrophage RAW264.7 cells and human T lymphoblast MOLT-4 cells with miR-223 mimics *in vitro*, respectively. As illustrated in Supporting Fig. S4A–B, overexpression of miR-223 did not attenuate rather than increase *Cd274* mRNA in macrophages nor affected PD-1 expression in T cells, suggesting that PD-1 and PD-L1 expression in immune cells are not directly targeted/inhibited by miR-223.

To explore the mechanisms by which miR-223 regulates tumor microenvironment in HCC, we searched the potential targets of miR-223 in HCC cells by comparing the gene profiles of HCC patients with high- and low- miR-223 expression (miR-223^{high} and miR-223^{low} groups) in the Cancer Genome Atlas database (Supporting Fig. S5A). Gene ontology enrichment analysis indicated that miR-223^{high} patients showed higher activation of several pathways including cellular response to oxygen levels compared to miR-223^{low} patients (Fig. 4A). Bioinformatic analysis predicts that hypoxia inducible factor-1α (*Hif-1a*), a master regulator for cellular response to hypoxia,²⁵ is a potential target of miR-223 (Supporting Fig. S5B). *In vitro* transfection of miR-223 markedly reduced luciferase activity of luciferase vector containing the 3' untranslated region (3'UTR) of *Hif1a* in Hepa1-6 cells (Supporting Fig. S5C) and decreased *Hif1a* mRNA/HIF-1α protein and its target CA9 expression (Fig. 4B, Supporting Fig. S5D), suggesting that HIF-1α is the target of miR-223 in HCC. Immunostaining analyses detected HIF-1α in nucleus of HCC in DEN+CCl₄ model with greater levels in miR-223KO mice than in WT mice (Fig. 4C). RT-qPCR and western blot analyses also detected higher *Hif-1a* mRNA and protein expression in the tumor region samples of miR-223KO mice than those in WT mice (Fig. 4D–E). In agreement with these data, several HIF-1α target genes were significantly higher in miR-223KO mice compared with WT mice in DEN+CCl₄ model (Fig. 4F). Meanwhile, the expression of *Pdcd1* or *Cd274* in non-tumor adjacent livers positively correlated with *Hif1a* expressed in HCC tumor samples from DEN+CCl₄ treated mice (Fig. 4G). A similar correlation was also observed between *HIF1A* (*HIF1A* encodes HIF-1α) and *PDCD1* or *CD274* in HCC patient samples from the TCGA cohort (Supporting Fig. S5E).

MiR-223 downregulates PD-1 and PD-L1 by limiting HIF-1 α in HCC cells in co-culture experiments

To investigate whether miR-223 inhibition of HIF-1 α in HCC cells regulates PD-1/PD-L1 in immune cells, we performed two types of experiments. First, the supernatants from Hepa1-6 cells transfected with miR-223 mimics or NC-mimics under normoxic or hypoxic conditions were added to primary mouse splenocytes or macrophages. Our data revealed that incubation with supernatant from miR-223 mimics-treated hypoxic Hepa1-6 cells downregulated *Pdcd1*/PD-1 and *Cd274*/PD-L1 expression in splenocytes and macrophages, respectively (Supporting Fig. S6A–C). Second, we conducted co-culture of primary CD3⁺ T cells or macrophages with Hepa1-6 cells transfected with miR-223 mimics or NC-mimics under normoxic and hypoxic conditions (The scheme is shown in Fig. 5A). Western blot and flow-cytometric analyses revealed that miR-223 reduced PD-1 and PD-L1 protein expression in T cells and macrophages, respectively, when these cells were co-cultured with hypoxic Hepa1-6 cells but did not affect their expression under normoxia condition (Fig. 5B–E, Supporting Fig. S6D–E).

MiR-223 inhibition of the HIF-1 α -CD39/CD73-adenosine pathway attenuates hypoxia-driven PD-1/PD-L1 activation, thus suppressing HCC development

The above data demonstrated that miR-223 regulates HIF-1 α in HCC cells and subsequently regulates PD-1/PD-L1 expression in immune cells. To investigate the link between HIF-1 α in HCC and PD-1/PD-L1 in immune cells, we focused on CD39 and CD73, two key ectonucleotides that have been proven to drive tumor immunosuppression by metabolizing ATP into adenosine.^{20–23} We firstly measured CD39/CD73 and adenosine levels in tumor regions in the DEN+CCl₄ model, and found their levels in HCC tissues were higher in miR-223KO mice *versus* WT mice (Fig. 6A). *In vitro* experiments (Supporting Fig. S7A) revealed that under hypoxia condition, HCC cells had elevated *Cd39/Cd73* expression, and such elevation was attenuated by miR-223 mimics. MiR-223 mimics did not affect *Cd39/Cd73* expression under normoxia. These data suggest that miR-223 attenuates *Cd39/Cd73* expression in HCC via the downregulation of HIF1 α . Previous studies have reported that *Cd39* and *Cd73* are direct target genes of HIF-1 α as demonstrated by chromatin immunoprecipitation (ChIP) assay.^{26–28} Here we also performed several experiments to support this notion. First, knockdown of *Hif1a* with shRNA transfection markedly reduced *Cd39* and *Cd73* expression in hypoxic Hepa1-6 cells (Supporting Fig. S7B). Second, ChIP assay revealed that HIF-1 α was recruited to the promoter regions of CD39 and CD73 under hypoxia (Supporting Fig. S7C), suggesting that HIF-1 α directly induces *Cd39/Cd73* expression in HCC.

Next, we performed *in vitro* experiments to test the hypothesis that CD39/CD73 in HCCs promote PD-1/PD-L1 expression in immune cells. *In vitro* treatment with the CD73 inhibitor AMP-CP reduced *Cd274*/PD-L1 and *Pdcd1*/PD-1 expression in primary macrophages and T cells co-cultured with hypoxic Hepa1-6 cells, respectively, while treatment with the CD39 inhibitor POM-1 had no effect (Supporting Fig. S7D). Furthermore, overexpression of miR-223 in Hepa1-6 cells under hypoxia suppressed the generation of adenosine (Fig. 6B). To define whether adenosine affects PD-1/PD-L1 activation, we treated primary T cells and macrophages with adenosine and A2A adenosine receptor inhibitor CPI-444. As illustrated

in Fig. 6C and Supporting Fig. S8A–B, treatment with adenosine significantly upregulated *Pdcd1*/PD-1 and *Cd274*/PD-L1 expression in T cells and macrophages, respectively, while co-treatment with CPI-444 diminished these elevations.

To examine whether the CD73-adenosine signaling is involved in HCC development by regulating PD-1/PD-L1 activation *in vivo*, we established an inflammation-related orthotopic HCC model by combining CCl₄ intervention and Hepa1-6 implantation (supporting Fig. S9A). Compared to Hepa1-6 alone orthotopic model, this model not only presented greater tumor growth with many PD-1⁺/PD-L1⁺ immune cell infiltration, but also developed more severe angiogenesis, inflammation and tumor hypoxia as evidenced by higher CD31, CD45 and HIF-1 α protein levels (Supporting Fig. S9B–F). Blockage of CD73 with anti-CD73 antibody markedly inhibited tumor growth and reduced the percentages of PD-1⁺ CD8⁺ T cells and PD-L1⁺ macrophages in this CCl₄ plus orthotopic HCC model (Fig. 6D–E). Finally, treatment with the A2A adenosine receptor inhibitor CPI-444 significantly reduced tumor size and the percentages of PD-1⁺ CD8⁺ T cells and exhibited tendency to decrease PD-L1⁺ macrophages percentage *in vivo* (Supporting Fig. S10A–B).

MiR-223 downregulates PD-1/PD-L1 and angiogenesis in tumor microenvironment by targeting HIF-1 α in HCC

To elucidate whether HIF-1 α induction in HCCs contributes to miR-223-mediated inhibition of PD-1/PD-L1 in immune cells *in vivo*, we knocked down *Hif1a* expression in Hepa1-6 cells by transfecting *Hif1a* shRNA, the knockdown efficiency is confirmed by RT-qPCR and western blot analyses (Supporting Fig. S11A–B). Hepa1-6 cells were then implanted in WT and miR-223KO mice for the orthotopic model establishment. As illustrated in Fig. 7A–D and supporting Fig. S11C–D, miR-223KO mice had greater tumor volume, more severe angiogenesis, higher expression levels of *Cd39*/*Cd73* and several pro-angiogenic genes (*Egfr*, *Endogli*, *Vegf*), and greater vascularization in tumor tissues than WT mice, such differences between WT and miR-223KO mice were diminished in *Hif1a* shRNA-transfected HCC experiments. In addition, immunostaining and RT-qPCR analyses revealed that *Hif1a* knockdown in HCC cells ameliorated *Pdcd1*/PD-1 and *Cd274*/PD-L1 expression, and PD-1⁺/PD-L1⁺ cell infiltration in tumor adjacent liver tissues in both WT and miR-223 KO mice (Fig. 7E–F, Supporting Fig. S11E).

Gene delivery of miR-223 ameliorates tumor angiogenesis, hypoxia, PD-1/PD-L1 expression and tumor proliferation

To test the therapeutic efficacy of miR-223 in HCC, we performed tail vein injection with adenovirus loaded miR-223 (Ad-miR-223) in the DEN+CCl₄ model (Supporting Fig. S12A). Compared with the control (adenovirus-GFP vector; Ad-GFP), Ad-miR-223 significantly decreased HCC growth as demonstrated by reduced number and size of the tumor mass (Fig. 8A–B). Immunofluorescence staining demonstrated the expression of CD31, PCNA, CA9 and Ki67 in tumor region was suppressed in Ad-miR-223-treated group compared to control Ad-GFP group (Fig. 8C–D, Supporting Fig. S12B). Western blot analysis revealed that injection of Ad-miR-223 ameliorated angiogenesis, proliferation and hypoxia of HCC tumor in the DEN+CCl₄ model, which was evidenced by reduced PCNA, HIF-1 α , and phosphorylated VEGFR2 and Tie2 (Fig. 8E–F). Meanwhile, administration of

Ad-miR-223 markedly decreased the expression of several HIF-1 α target genes (Fig. 9A). In addition, we found that the percentage of PD-1⁺ CD8⁺ T cells, and PD-L1⁺ macrophages (IBA1⁺ cells) in tumor adjacent region, was lower in Ad-miR-223 treated mice than those in control Ad-GFP group (Fig. 9B). As expected, Ad-miR-223 decreased fibrosis and chronic inflammation in tumor microenvironment of HCC (Supporting Fig. S12C).

We also tested the therapeutic efficacy of miR-223 in HCCs by using the inflammation-associated orthotopic HCC mouse model. Notably, injection of Ad-miR-223 markedly reduced progression of HCC (Fig. 10A–B). RT-PCR analyses confirmed the upregulated miR-223 in the HCC region of mice after Ad-miR-223 injection (Fig. 10C). Immunostaining analysis also confirmed the successful injection of Ad-miR-223 (labelled with GFP) (Supporting Fig. S13A). Western blot analysis demonstrated that treatment with Ad-miR-223 markedly reduced tumor cell proliferation, angiogenesis, and hypoxia as evidenced by lower protein levels of HIF-1 α , PCNA and p-VEGFR2 in the Ad-miR-223 group than those in the Ad-GFP group (Fig. 10D–E). Immunostaining also demonstrated that treatment with Ad-miR-223 reduced the expression of angiogenesis marker CD31, cell proliferation marker Ki67, and decreased PD-1⁺/PD-L1⁺ cell infiltration in the inflammation-associated orthotopic HCC mouse model (Fig. 10F).

Discussion

In the present study, we identified miR-223 as a key orchestrator for tumor hypoxia and inflammatory tumor microenvironment in controlling HCC progression. Mechanistically, HIF-1 α is a direct target of miR-223 in HCC, and miR-223 ameliorates HCC growth, angiogenesis and PD-1/PD-L1 activation in HCC surrounding regions by limiting HIF-1 α . The therapeutic potential of miR-223 was tested in two mouse models of HCC with chronic liver inflammation. Collectively, we present a model depicting an important anti-HCC effect of miR-223 by modulating HCC hypoxia, immunosuppression, and angiogenesis (Fig. 11).

Abnormal expression of miR-223 is well-documented in many malignancies and miR-223 has been regarded as a biomarker for early-stage screening or diagnosis in various types of cancers.^{29, 30} In HCC, miR-223 was found to be preferentially expressed in EpCAM⁺ HCC cells³¹ but was markedly reduced in tumor tissues compared with adjacent non-tumoral livers.¹⁶ Several *in vitro* studies using cultured cells suggest that miR-223 exerts tumor suppressor functions by regulating *STMN1* and *FOXO1* in HCC.^{15, 32} However, it remains unknown whether and how miR-223 regulates tumor environment and HCC progression *in vivo*. This question was investigated in the current study by using two clinically relevant mouse models of HCC. Our data revealed an important role of miR-223 in attenuating HCC progression by regulating angiogenesis and immune checkpoint. First, deletion of miR-223 exacerbated chronic inflammation, liver fibrosis and HCC growth. Second, deletion of miR-223 upregulated pro-angiogenic responses as evidenced by elevation of endothelial cell marker CD31, angiogenesis related genes (*Endoglin*, *Vegf*), and phosphorylated VEGFR2. The miR-223 deficiency-associated angiogenesis may also contribute to the increased PD-1⁺ and PD-L1⁺ immune cell infiltration in miR-223KO mice in addition to the well-documented miR-223-mediated direct inhibition of immune cell infiltration.¹⁴ Third, deletion of miR-223 markedly promoted tumor immunosuppression by enhancing

infiltration of PD-1⁺ T cells and PD-L1⁺ macrophages surrounding HCC tumor tissues, suggesting miR-223 acts an immune checkpoint blockade to control HCC progression. To our surprise, overexpression of miR-223 did not directly inhibit PD-1 and PD-L1 expression in T cells and macrophages, respectively. These data suggest that miR-223 regulates PD-1 and PD-L1 expression in immune cells during HCC development via an indirect mechanism. Our subsequent study suggests that miR-223 directly targets HIF-1 α in HCC and modulate tumor hypoxia microenvironment, thereby limiting angiogenesis and PD-1/PD-L1 expression.

Hypoxia has been strongly linked to enhanced tumor progression, angiogenesis and poor clinical outcomes.^{33–35} As a key regulator of hypoxia, HIF-1 α contributes to HCC development by regulating USP22 and SENP1 to control HCC tumor growth^{36, 37} and upregulating angiogenesis related genes.³⁸ Emerging data suggest that HIF-1 α modulates immune microenvironment to promote HCC by inducing myeloid-derived suppressor cell accumulation and cytokine secretion,^{39, 40} by causing T cell exhaustion, and modulating the PD-1/PD-L1 pathway.^{41–44} However, it is still obscure how HIF-1 α , which is regulated by miR-223, orchestrates pro-angiogenic and immunosuppressive tumor environment in HCC. HIF-1 α complex is known to be mainly regulated post-translationally in response to oxygen level,⁴⁴ our data that *Hif1a* gene is a direct target of miR-223 add an additional important mechanism regulating HIF-1 expression at mRNA levels in HCC. Downregulation of *Hif1a* mRNA is consistent with downregulation of HIF-1 α protein and its downstream target genes by miR-223 in HCC, as demonstrated in the current study. In addition, we provided several lines of evidence suggesting that miR-223 downregulates the HIF- α -CD39/CD73-adenosine pathway in HCC, and subsequently abolishes adenosine-mediated upregulation of PD-1 and PD-L1 in immune cells. First, CD39/CD73 and adenosine levels in HCC were higher in miR-223KO mice compared to WT mice in DEN+CCl₄ induced HCC. Second, overexpression of miR-223 reduces expression of CD39/CD73 and adenosine concentrations in the supernatant of Hepa1-6 cells under hypoxia. Third, treatment with adenosine upregulates *Pdcd1/Cd274* expression in immune cells. Finally, *in vivo* treatment with CD73 antibody or A2A adenosine receptor inhibitor reduced *Pdcd1/Cd274* expression and tumor size in inflammation-associated Hepa1-6-transplanted HCC model. In addition to regulation of the CD39/CD73-adenosine pathway, HIF-1 α also induces many other immunosuppressive genes to promote immunosuppressive environment,^{41–44} whether these genes also contribute to HIF-1 α -mediated immunosuppression in our HCC models deserves further studies.

MiR-223 is mainly expressed in myeloid cells (especially neutrophils) with low expression in hepatocytes,¹⁰ but it can be transferred from myeloid cells into hepatocytes via extracellular vesicles (EVs); thereby inhibiting expression of proinflammatory and fibrotic genes in hepatocytes.^{11, 45} In the current study, we found that a large number of infiltrating neutrophils were detected in tumor adjacent regions, which may partially explain lower miR-223 expression in tumor tissues compared to neutrophils-enriched adjacent non-tumor liver tissues, both in mouse model and human HCC samples. Additionally, we found that HCC cells were able to take up neutrophils-derived EVs and miR-223 (Supporting Figure S13B–C). Thus, we speculate that infiltrated myeloid cells may transfer miR-223 into HCCs

and subsequently inhibit HIF-1 α and modulate tumor microenvironment; however, future studies using cell-specific miR-223KO mice are required to confirm this speculation.

Clinical significance of the current study.

Recent clinical trials of anti-PD-1/PD-L1 immune checkpoint inhibitors have offered a promising future for cancer patients. For HCC clinical therapy, considerable efforts are underway to improve the efficacy of immunotherapy. Emerging evidence revealed that the combination of PD-1/PD-L1 inhibitors and anti-angiogenic regimens, such as multi-kinase inhibitors and VEGF targeted agents showed better benefits and encouraging clinical efficacy for HCC treatment.^{46, 47} In our current study, we found adenovirus miR-223 gene therapy significantly hindered HCC development by limiting chronic inflammation, PD-1/PD-L1-mediated immune escape and tumor angiogenesis in two mouse models of inflammation-associated HCC, which is partially mediated via the direct inhibition of HIF-1 α in tumor tissues. It is known that injection of adenovirus miR-223 also transduces hepatocytes but very unlikely transduces immune cells, and miR-223 has been shown to inhibit the expression of multiple inflammatory and fibrogenic genes in liver.^{12, 14, 48} Thus, gene delivery of miR-223 in hepatocytes may generate additional anti-inflammatory and anti-fibrotic benefits during anti-HCC therapy. Since miR-223 is markedly downregulated in HCC,¹⁵ it is plausible that restoration of miR-223 in HCC may improve the efficacy of the current combination therapy for HCC with PD-1/PD-L1 inhibitors and anti-angiogenic regimens.

Supplementary Material

Refer to Web version on PubMed Central for supplementary material.

Acknowledgment:

The authors want to thank Dr. Tim Greten (NCI, NIH) for his valuable comments and critical reading the manuscript.

Grant support:

This work was supported by the intramural program of NIAAA, NIH (B.G.).

References:

1. Hanahan D, Weinberg RA. Hallmarks of cancer: the next generation. *Cell* 2011;144:646–74. [PubMed: 21376230]
2. Finn RS, Qin S, Ikeda M, et al. Atezolizumab plus Bevacizumab in Unresectable Hepatocellular Carcinoma. *N Engl J Med* 2020;382:1894–1905. [PubMed: 32402160]
3. Sengez B, Carr BI, Alotaibi H. EMT and Inflammation: Crossroads in HCC. *J Gastrointest Cancer* 2022.
4. Yang YM, Kim SY, Seki E. Inflammation and Liver Cancer: Molecular Mechanisms and Therapeutic Targets. *Semin Liver Dis* 2019;39:26–42. [PubMed: 30809789]
5. Geh D, Leslie J, Rumney R, et al. Neutrophils as potential therapeutic targets in hepatocellular carcinoma. *Nat Rev Gastroenterol Hepatol* 2022;19:257–273. [PubMed: 35022608]
6. Leslie J, Mackey JBG, Jamieson T, et al. CXCR2 inhibition enables NASH-HCC immunotherapy. *Gut* 2022;71:2093–106. [PubMed: 35477863]

7. Dudek M, Tacke F. Immature neutrophils bring anti-PD-1 therapy in NASH-HCC to maturity. *Gut* 2022.
8. Wu C, Lin J, Weng Y, et al. Myeloid signature reveals immune contexture and predicts the prognosis of hepatocellular carcinoma. *J Clin Invest* 2020;130:4679–4693. [PubMed: 32497024]
9. Wang X, He Y, Mackowiak B, et al. MicroRNAs as regulators, biomarkers and therapeutic targets in liver diseases. *Gut* 2021;70:784–795. [PubMed: 33127832]
10. Li M, He Y, Zhou Z, et al. MicroRNA-223 ameliorates alcoholic liver injury by inhibiting the IL-6-p47(phox)-oxidative stress pathway in neutrophils. *Gut* 2017;66:705–715. [PubMed: 27679493]
11. Calvente CJ, Tameda M, Johnson CD, et al. Neutrophils contribute to spontaneous resolution of liver inflammation and fibrosis via microRNA-223. *J Clin Invest* 2019;130:4091–4109.
12. Jimenez Calvente C, Del Pilar H, Tameda M, et al. MicroRNA 223 3p Negatively Regulates the NLRP3 Inflammasome in Acute and Chronic Liver Injury. *Mol Ther* 2020;28:653–663. [PubMed: 31585800]
13. He Y, Feng D, Li M, et al. Hepatic mitochondrial DNA/Toll-like receptor 9/MicroRNA-223 forms a negative feedback loop to limit neutrophil overactivation and acetaminophen hepatotoxicity in mice. *Hepatology* 2017;66:220–234. [PubMed: 28295449]
14. He Y, Hwang S, Cai Y, et al. MicroRNA-223 Ameliorates Nonalcoholic Steatohepatitis and Cancer by Targeting Multiple Inflammatory and Oncogenic Genes in Hepatocytes. *Hepatology* 2019;70:1150–1167. [PubMed: 30964207]
15. Wong QW, Lung RW, Law PT, et al. MicroRNA-223 is commonly repressed in hepatocellular carcinoma and potentiates expression of Stathmin1. *Gastroenterology* 2008;135:257–69. [PubMed: 18555017]
16. Dong YW, Wang R, Cai QQ, et al. Sulfatide epigenetically regulates miR-223 and promotes the migration of human hepatocellular carcinoma cells. *J Hepatol* 2014;60:792–801. [PubMed: 24333181]
17. Pratedrat P, Chuaypen N, Nimsamer P, et al. Diagnostic and prognostic roles of circulating miRNA-223–3p in hepatitis B virus-related hepatocellular carcinoma. *PLoS One* 2020;15:e0232211. [PubMed: 32330203]
18. Zhou J, Yu L, Gao X, et al. Plasma microRNA panel to diagnose hepatitis B virus-related hepatocellular carcinoma. *J Clin Oncol* 2011;29:4781–8. [PubMed: 22105822]
19. Caviglia JM, Schwabe RF. Mouse models of liver cancer. *Methods Mol Biol* 2015;1267:165–83. [PubMed: 25636469]
20. Vijayan D, Young A, Teng MWL, et al. Targeting immunosuppressive adenosine in cancer. *Nat Rev Cancer* 2017;17:709–724. [PubMed: 29059149]
21. Allard B, Allard D, Buisseret L, et al. The adenosine pathway in immuno-oncology. *Nat Rev Clin Oncol* 2020;17:611–629. [PubMed: 32514148]
22. Thompson EA, Powell JD. Inhibition of the Adenosine Pathway to Potentiate Cancer Immunotherapy: Potential for Combinatorial Approaches. *Annu Rev Med* 2021;72:331–348. [PubMed: 32903139]
23. Allard B, Longhi MS, Robson SC, et al. The ectonucleotidases CD39 and CD73: Novel checkpoint inhibitor targets. *Immunol Rev* 2017;276:121–144. [PubMed: 28258700]
24. Fu Y, Liu S, Rodrigues RM, et al. Activation of VIPR1 suppresses hepatocellular carcinoma progression by regulating arginine and pyrimidine metabolism. *Int J Biol Sci* 2022;18:4341–4356. [PubMed: 35864952]
25. Semenza GL. Targeting HIF-1 for cancer therapy. *Nat Rev Cancer* 2003;3:721–32. [PubMed: 13130303]
26. Pang L, Ng KT, Liu J, et al. Plasmacytoid dendritic cells recruited by HIF-1alpha/eADO/ADORA1 signaling induce immunosuppression in hepatocellular carcinoma. *Cancer Lett* 2021;522:80–92. [PubMed: 34536555]
27. Synnestvedt K, Furuta GT, Comerford KM, et al. Ecto-5'-nucleotidase (CD73) regulation by hypoxia-inducible factor-1 mediates permeability changes in intestinal epithelia. *J Clin Invest* 2002;110:993–1002. [PubMed: 12370277]

28. Tak E, Jung DH, Kim SH, et al. Protective role of hypoxia-inducible factor-1alpha-dependent CD39 and CD73 in fulminant acute liver failure. *Toxicol Appl Pharmacol* 2017;314:72–81. [PubMed: 27899277]
29. Haneklaus M, Gerlic M, O'Neill LA, et al. miR-223: infection, inflammation and cancer. *J Intern Med* 2013;274:215–26. [PubMed: 23772809]
30. Aalami AH, Abdeahad H, Mesgari M, et al. MicroRNA-223 in gastrointestinal cancers: A systematic review and diagnostic meta-analysis. *Eur J Clin Invest* 2021;51:e13448. [PubMed: 33244751]
31. Ji J, Zheng X, Forgues M, et al. Identification of microRNAs specific for epithelial cell adhesion molecule-positive tumor cells in hepatocellular carcinoma. *Hepatology* 2015;62:829–40. [PubMed: 25953724]
32. Wu L, Li H, Jia CY, et al. MicroRNA-223 regulates FOXO1 expression and cell proliferation. *FEBS Lett* 2012;586:1038–43. [PubMed: 22569260]
33. Li J, Xu Y, Long XD, et al. Cbx4 governs HIF-1alpha to potentiate angiogenesis of hepatocellular carcinoma by its SUMO E3 ligase activity. *Cancer Cell* 2014;25:118–31. [PubMed: 24434214]
34. Yuen VW, Wong CC. Hypoxia-inducible factors and innate immunity in liver cancer. *J Clin Invest* 2020;130:5052–5062. [PubMed: 32750043]
35. Ma L, Craig AJ, Heinrich S. Hypoxia is a key regulator in liver cancer progression. *J Hepatol* 2021;75:736–737. [PubMed: 34097995]
36. Cui CP, Wong CC, Kai AK, et al. SENP1 promotes hypoxia-induced cancer stemness by HIF-1alpha deSUMOylation and SENP1/HIF-1alpha positive feedback loop. *Gut* 2017;66:2149–2159. [PubMed: 28258134]
37. Ling S, Shan Q, Zhan Q, et al. USP22 promotes hypoxia-induced hepatocellular carcinoma stemness by a HIF1alpha/USP22 positive feedback loop upon TP53 inactivation. *Gut* 2020;69:1322–1334. [PubMed: 31776228]
38. de Heer EC, Jalving M, Harris AL. HIFs, angiogenesis, and metabolism: elusive enemies in breast cancer. *J Clin Invest* 2020;130:5074–5087. [PubMed: 32870818]
39. Chiu DK, Tse AP, Xu IM, et al. Hypoxia inducible factor HIF-1 promotes myeloid-derived suppressor cells accumulation through ENTPD2/CD39L1 in hepatocellular carcinoma. *Nat Commun* 2017;8:517. [PubMed: 28894087]
40. Ye LY, Chen W, Bai XL, et al. Hypoxia-Induced Epithelial-to-Mesenchymal Transition in Hepatocellular Carcinoma Induces an Immunosuppressive Tumor Microenvironment to Promote Metastasis. *Cancer Res* 2016;76:818–30. [PubMed: 26837767]
41. Shurin MR, Umansky V. Cross-talk between HIF and PD-1/PD-L1 pathways in carcinogenesis and therapy. *J Clin Invest* 2022;132.
42. Bailey CM, Liu Y, Liu M, et al. Targeting HIF-1alpha abrogates PD-L1-mediated immune evasion in tumor microenvironment but promotes tolerance in normal tissues. *J Clin Invest* 2022;132.
43. Salman S, Meyers DJ, Wicks EE, et al. HIF inhibitor 32–134D eradicates murine hepatocellular carcinoma in combination with anti-PD1 therapy. *J Clin Invest* 2022;132.
44. Wicks EE, Semenza GL. Hypoxia-inducible factors: cancer progression and clinical translation. *J Clin Invest* 2022;132.
45. He Y, Rodrigues RM, Wang X, et al. Neutrophil-to-hepatocyte communication via LDLR-dependent miR-223-enriched extracellular vesicle transfer ameliorates nonalcoholic steatohepatitis. *J Clin Invest* 2021;131.
46. Lee MS, Ryoo BY, Hsu CH, et al. Atezolizumab with or without bevacizumab in unresectable hepatocellular carcinoma (GO30140): an open-label, multicentre, phase 1b study. *Lancet Oncol* 2020;21:808–820. [PubMed: 32502443]
47. Galle PR, Finn RS, Qin S, et al. Patient-reported outcomes with atezolizumab plus bevacizumab versus sorafenib in patients with unresectable hepatocellular carcinoma (IMbrave150): an open-label, randomised, phase 3 trial. *Lancet Oncol* 2021;22:991–1001. [PubMed: 34051880]
48. Wang X, Seo W, Park SH, et al. MicroRNA-223 restricts liver fibrosis by inhibiting the TAZ-IHH-GLI2 and PDGF signaling pathways via the crosstalk of multiple liver cell types. *Int J Biol Sci* 2021;17:1153–1167. [PubMed: 33867837]

What is already known on this topic

MiR-223 has anti-inflammatory and anti-fibrotic functions in liver disease.

MiR-223 expression is downregulated in HCC

What this study adds

MiR-223 inhibits hepatocarcinogenesis by modulating tumor microenvironment

MiR-223 attenuates hypoxia-induced tumor immunosuppression and angiogenesis in HCC via the inhibition of HIF-1 α

How this study might affect research, practice or policy

Restoration of miR-223 in HCC may improve the efficacy of the current combination therapy for HCC with PD-1/PD-L1 inhibitors and anti-angiogenic regimens

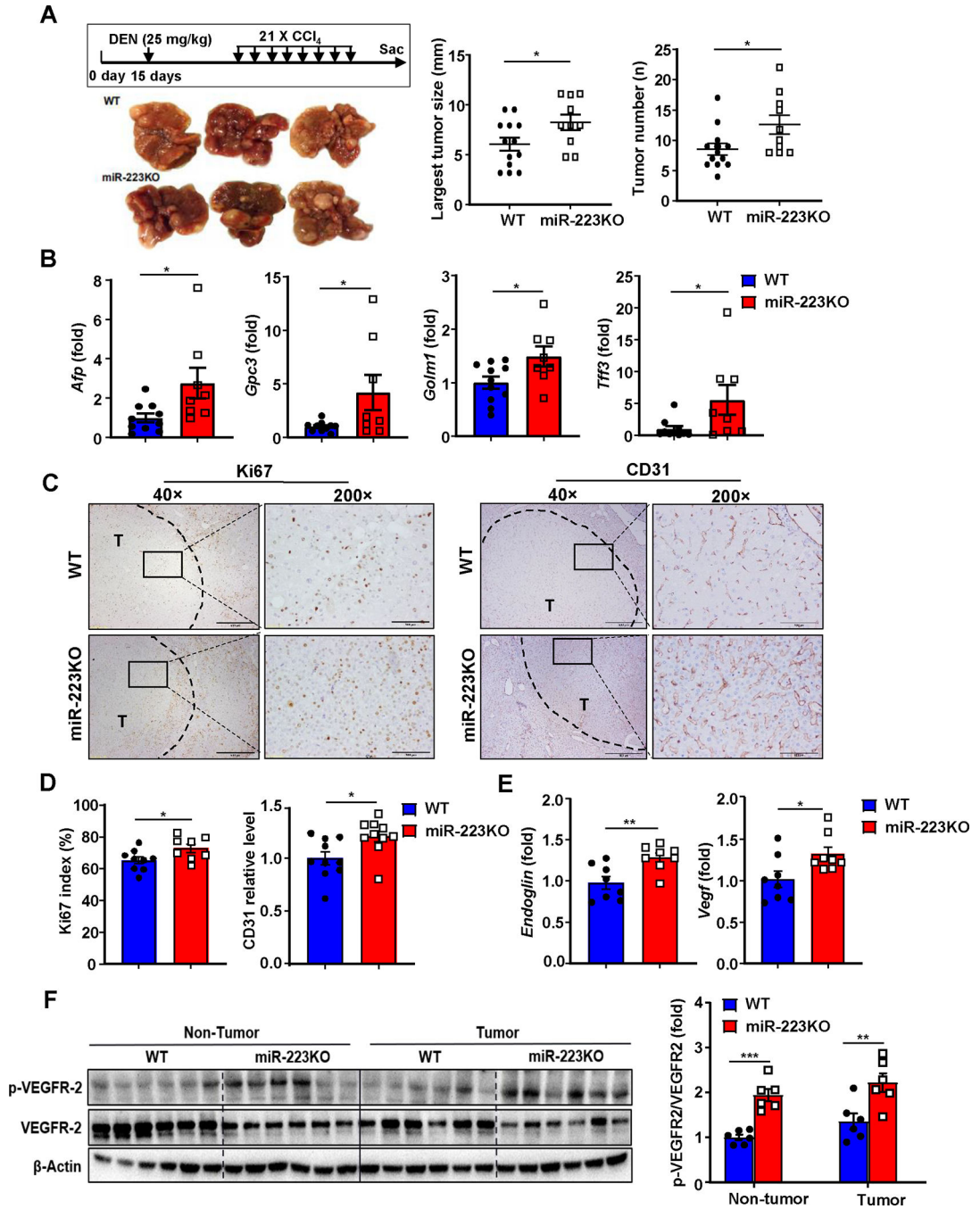


Figure 1. MiR-223 deficiency exacerbates HCC development and angiogenesis.

(A) Scheme of DEN+CCl₄-induced HCC mouse model (see details in methods).

Representative gross images of livers from miR-223KO and WT mice post DEN+CCl₄ treatment are shown. The largest tumor diameter and the number of tumor masses were calculated (right panel). (B) RT-qPCR analyses of HCC markers including *Afp*, *Gpc3*, *Golm2*, and *Tff3* in samples from miR-223KO and WT mice after DEN+CCl₄. (C) Representative images of Ki-67 and CD31 staining in livers from miR-223KO and WT mice are shown. Tumor region was surrounded by dashed line (T: tumor region). (D)

Ki-67 positive cells were counted and quantified as proliferation index; CD31 staining was quantified as the percentage of positive area in the whole section area. (E) RT-qPCR analyses of angiogenesis-related genes *Endoglin* and *Vegf* in HCC samples from miR-223KO and WT mice. (F) Western blot analysis of VEGFR2 and phosphorylated VEGFR-2 in non-tumor and tumor samples. Relative p-VEGFR2 protein levels were quantified. Values represent means \pm SEM. * $P < 0.05$, ** $P < 0.01$, *** $P < 0.001$.

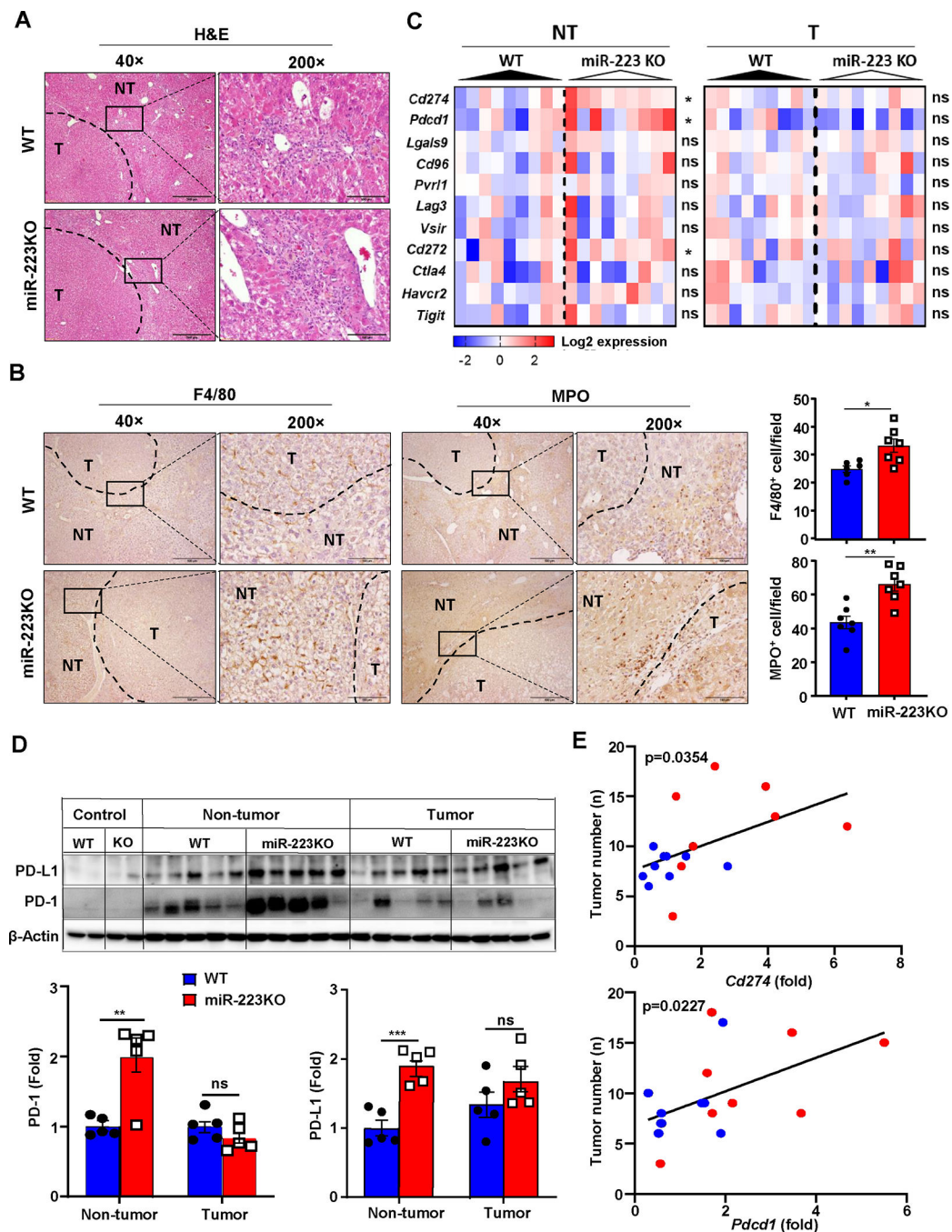


Figure 2. MiR-223 deficiency promotes inflammation-associated tumor immunosuppression and PD-1/PD-L1 expression.

WT and miR-223KO mice were challenged with DEN+CCl₄ as described in Figure 1. (A) Representative images of H&E staining in livers from miR-223KO and WT mice are shown. The tumor region was surrounded by dashed line (NT: non-tumor region; T: tumor region). (B) Representative images of F4/80 and MPO staining in non-tumor and tumor regions are shown. F4/80⁺ and MPO⁺ cells per field (x200) were quantified. (C) The expression levels of targeted immune checkpoint molecules in non-tumor (NT) and tumor (T) samples were analyzed by RT-qPCR analyses. (D) Western blot analysis PD-1 and PD-L1 proteins

in control healthy livers, tumor and adjacent non-tumor samples. (E) Correlation between *Pdcd1* or *Cd274* expression levels and tumor number in DEN+CCl₄-treated WT (n=14, blue dots) and miR-223KO mice (n=9, red dots) was analyzed. Values represent means \pm SEM. * $P < 0.05$, ** $P < 0.01$, *** $P < 0.001$.

Author Manuscript

Author Manuscript

Author Manuscript

Author Manuscript

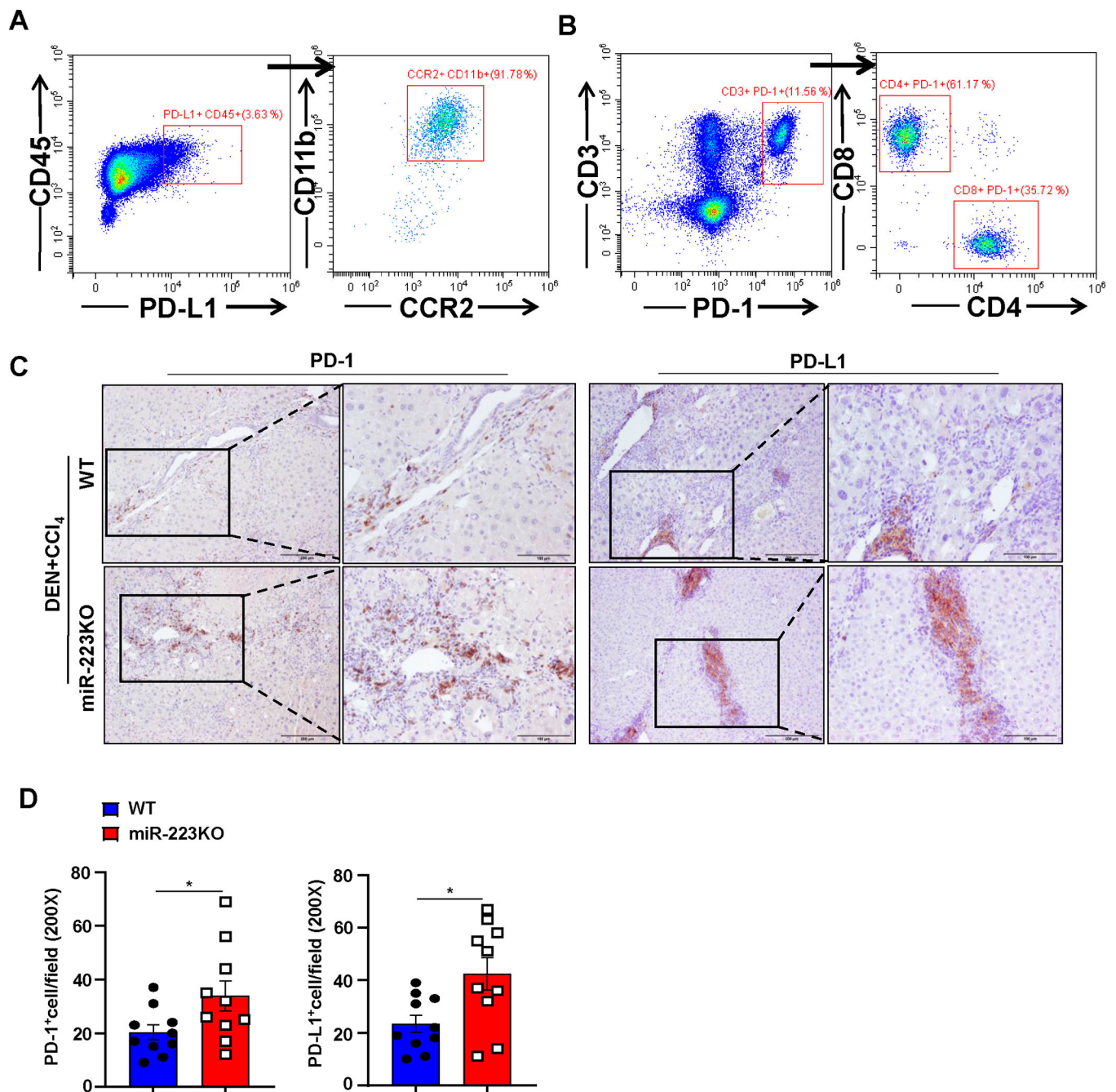


Figure 3. MiR-223KO mice have higher PD-1⁺T cells and PD-L1⁺macrophages than WT mice in DEN+CCl₄-induced HCC.

WT and miR-223KO mice were treated with DEN+CCl₄ as described in Figure 1. (A, B) Mouse livers from DEN+CCl₄-induced HCC were dissociated, PD-1⁺ or PD-L1⁺ cells were determined by flow cytometry. PD-L1 and PD-1 expression were mainly detected in CD11b⁺ CCR2⁺ macrophages (panel A) and CD4⁺/CD8⁺ T cells (panel B), respectively. (C, D) Representative images of PD-1 and PD-L1 staining of tumor and adjacent non-tumor samples from DEN+CCl₄ are shown in panel C. PD-1⁺ and PD-L1⁺ cells per field were quantified and are shown in panel D. Values represent means ± SEM. *P < 0.05.

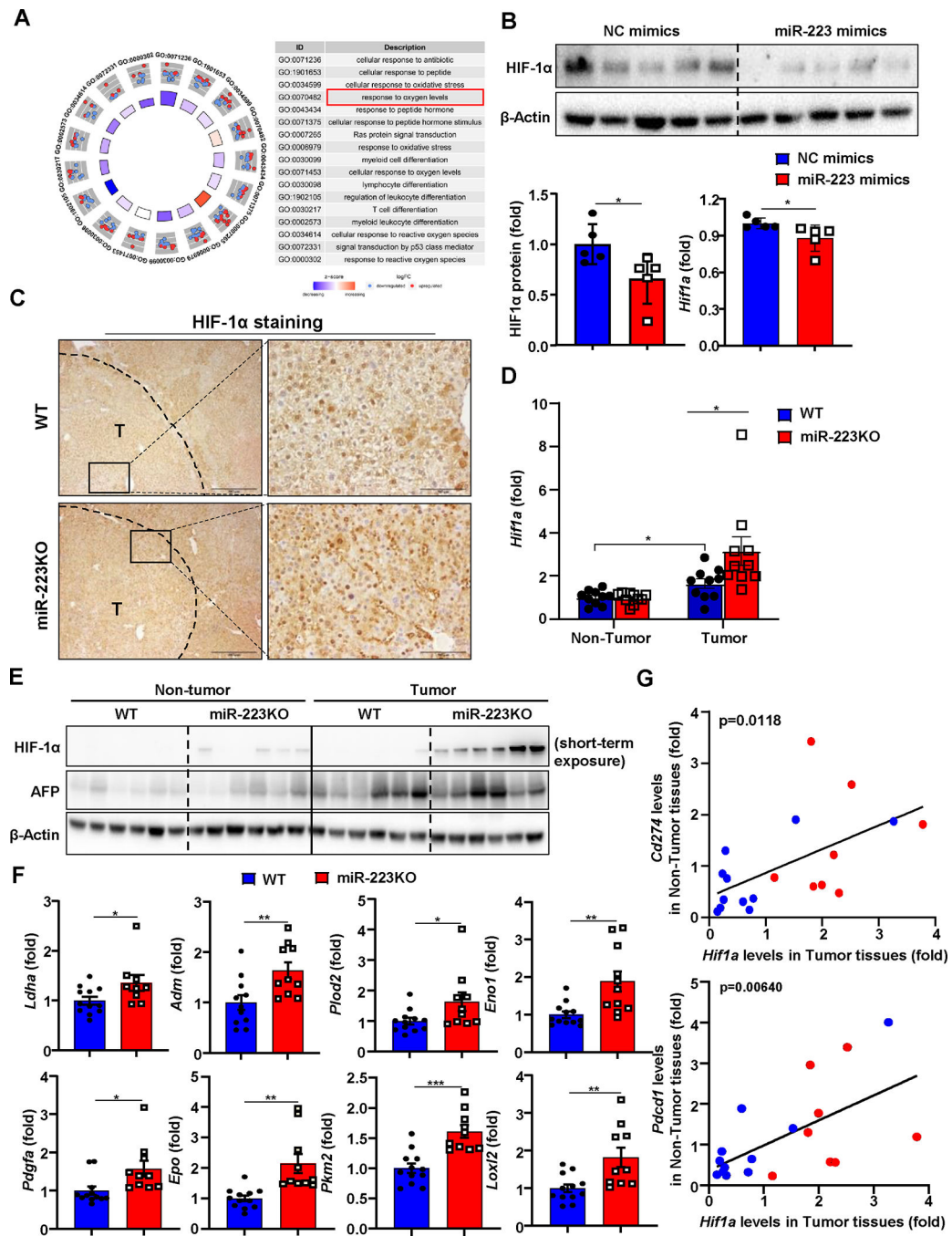


Figure 4. HIF-1 α in HCC cells is a direct downstream target of miR-223.

(A) Gene Ontology (GO) analysis was performed to compare the difference of gene profiling between miR-223^{high} and miR-223^{low} HCC patients in TCGA database, and the results are shown on the right side. (B) Measurement of HIF-1 α protein levels by western blot in Hepa1-6 cell after miR-223 mimics transfection. HIF-1 α protein levels were quantified (lower left panel). RT-qPCR was performed to determine *Hif1a* mRNA expression in Hepa1-6 cell after miR-223 mimics transfection (lower right panel). (C) WT and miR-223KO mice were treated with DEN+CCl₄ as described in Figure 1. Representative

images of HIF-1 α staining in HCC samples from miR-223KO and WT mice are shown. Tumor region was surrounded by dashed line (T: tumor region). (D, E) Tumor and adjacent non-tumor samples from miR-223KO and WT mice were subjected to RT-qPCR (panel D) and western blot analysis (panel E). (F) RT-qPCR analyses of HIF-1 α target genes in samples from miR-223KO and WT mice after DEN+CCl₄. (G) Correlation analysis of *Hif1a* expression in tumor samples and PD-1/PD-L1 (*Pdcd1/Cd274*) expression in non-tumor (NT) adjacent liver tissues from DEN+CCl₄ challenged WT (n=11; blue dots) and miR-223KO (n=8; red dots) mice. The average value from WT mice was set as 1. Values represent means \pm SEM. * P < 0.05, ** P < 0.01, *** P < 0.001.

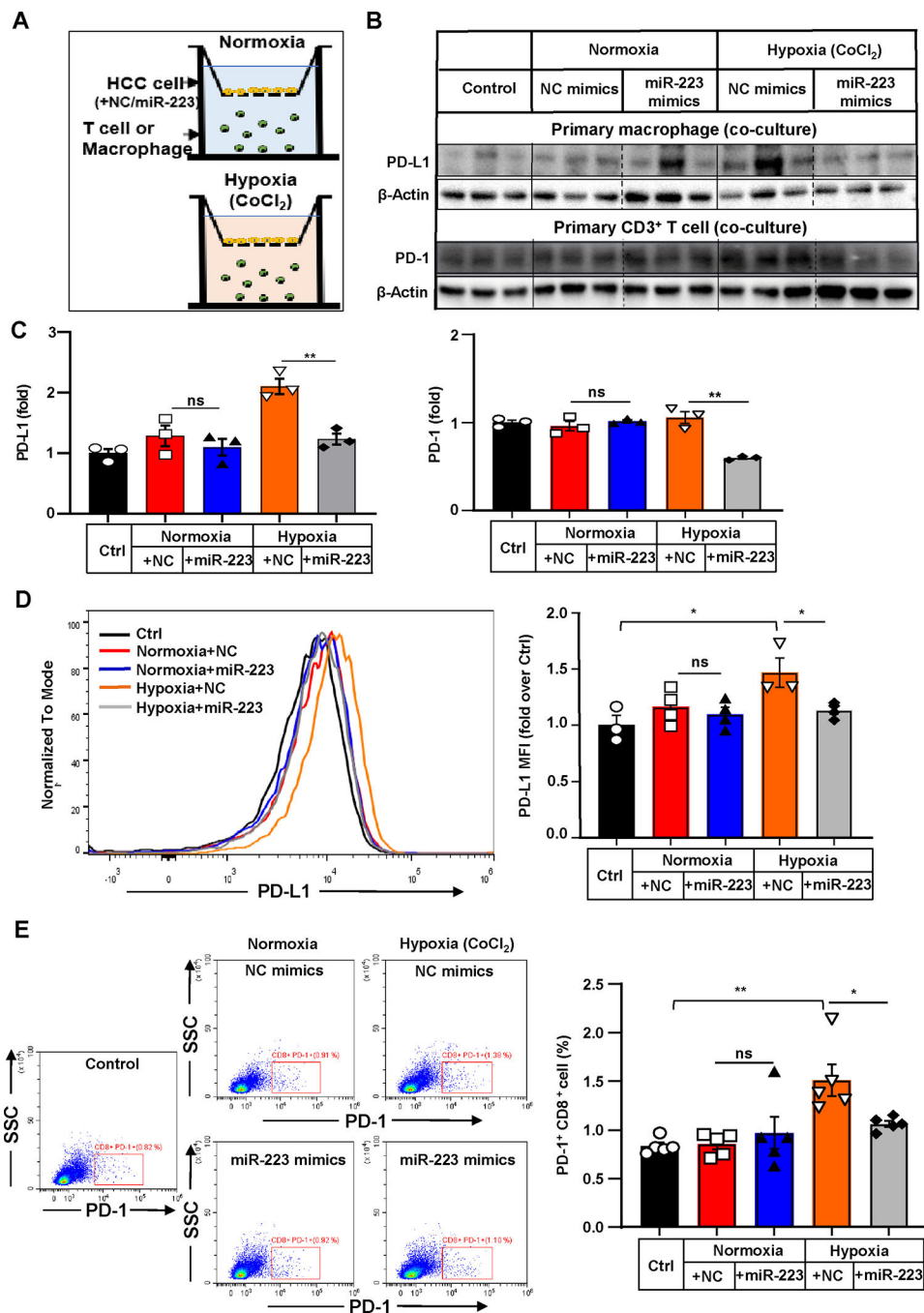


Figure 5. MiR-223 downregulates PD-1 and PD-L1 expression by targeting HIF-1 α -mediated hypoxia in HCC.

(A) Scheme of co-culture of primary T cells or macrophages with Hepa1-6 cells under normoxia and CoCl₂-induced hypoxia. Hepa1-6 cells were transfected with miR-223/NC mimics *in vitro* prior to establishment of co-culture system. (B, C) PD-1 expression in T cells or PD-L1 expression in macrophages were determined and quantified by western blot analysis. T cells or macrophages without any stimuli were set as control. (D) Representative flow cytometry analysis and quantification of PD-L1 expression of co-cultured primary macrophages. Mean Fluorescent Intensity (MFI) of PD-L1 was quantitated.

(E) Representative flow cytometry analysis of PD-1 expression of co-cultured T cells. The percentage of PD-1⁺ cells was quantified. Values represent means \pm SEM. * P < 0.05, ** P < 0.01.

Author Manuscript

Author Manuscript

Author Manuscript

Author Manuscript

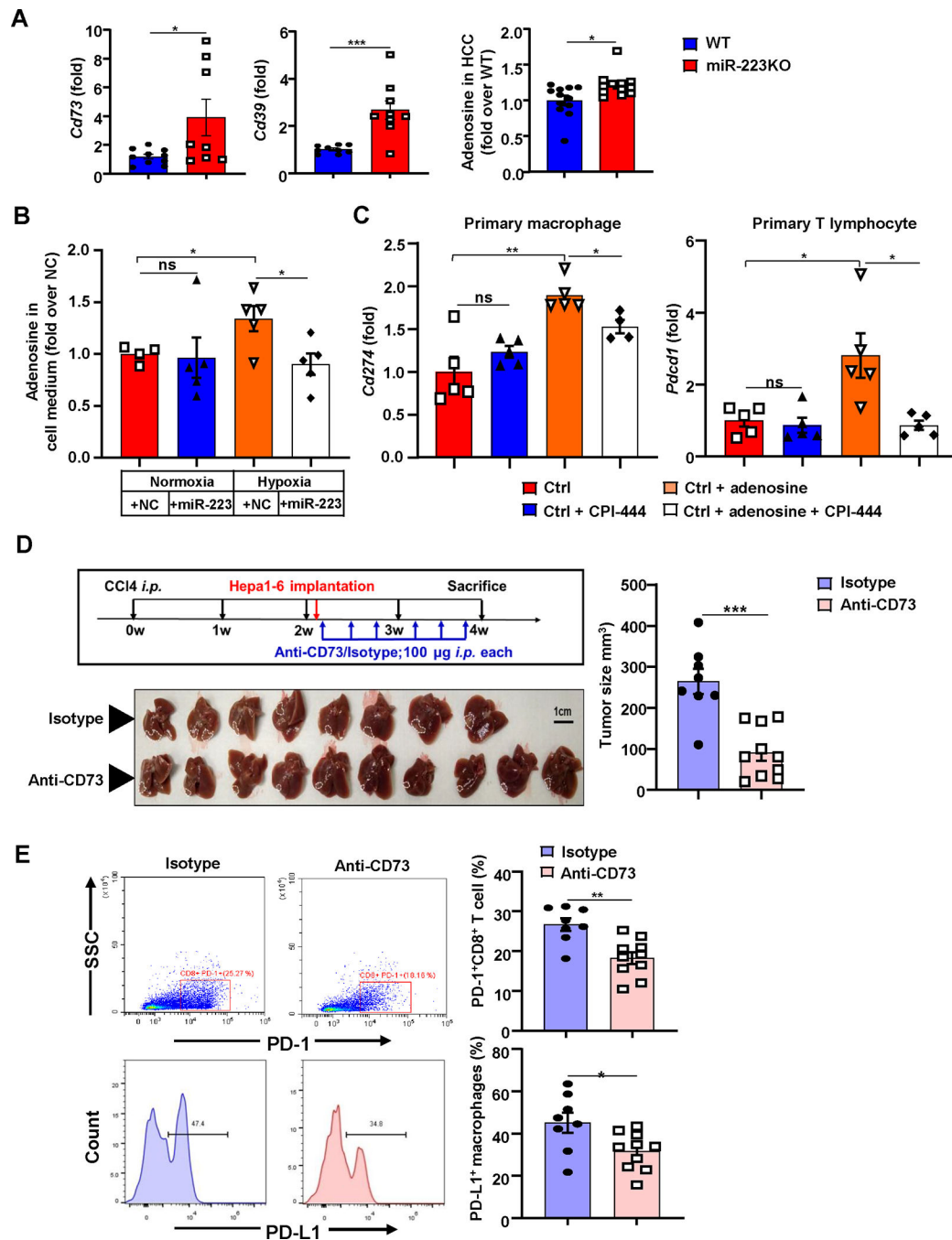


Figure 6. Inhibition of the CD39/CD73-adenosine pathway ameliorates hypoxia-driven immunosuppression in HCC development.

(A) WT and miR-223KO mice were treated with DEN+CCl₄ as described in Figure 1. Levels of extracellular adenosine ectonucleotidases *Cd39* and *Cd73* mRNA expression, and adenosine levels in HCC tissues from WT and miR-223KO mice were determined. (B) The relative adenosine levels in cell medium were analyzed in Hepa1-6 cells after miR-223/NC mimics transfection under normoxia and hypoxia. (C) Adenosine and/or A2A adenosine receptor inhibitor CPI-444 were applied in primary macrophages or primary T cells, *Cd274* and *Pdcd1* mRNA expression were determined by RT-qPCR. (D, E) C57BL/6J mice were

subjected to CCl₄+Hepa1-6-derived HCC model and treated with anti-CD73 (n=10) or isotype antibodies (n=8). Gross images of livers are shown, and tumor volume (mm³) was measured (panel D). The percentages of PD-1⁺CD8⁺ T cells and PD-L1⁺ macrophages were analyzed by flow cytometry (panel E). Values represent means ± SEM. **P* < 0.05, ***P* < 0.01, ****P* < 0.001.

Author Manuscript

Author Manuscript

Author Manuscript

Author Manuscript

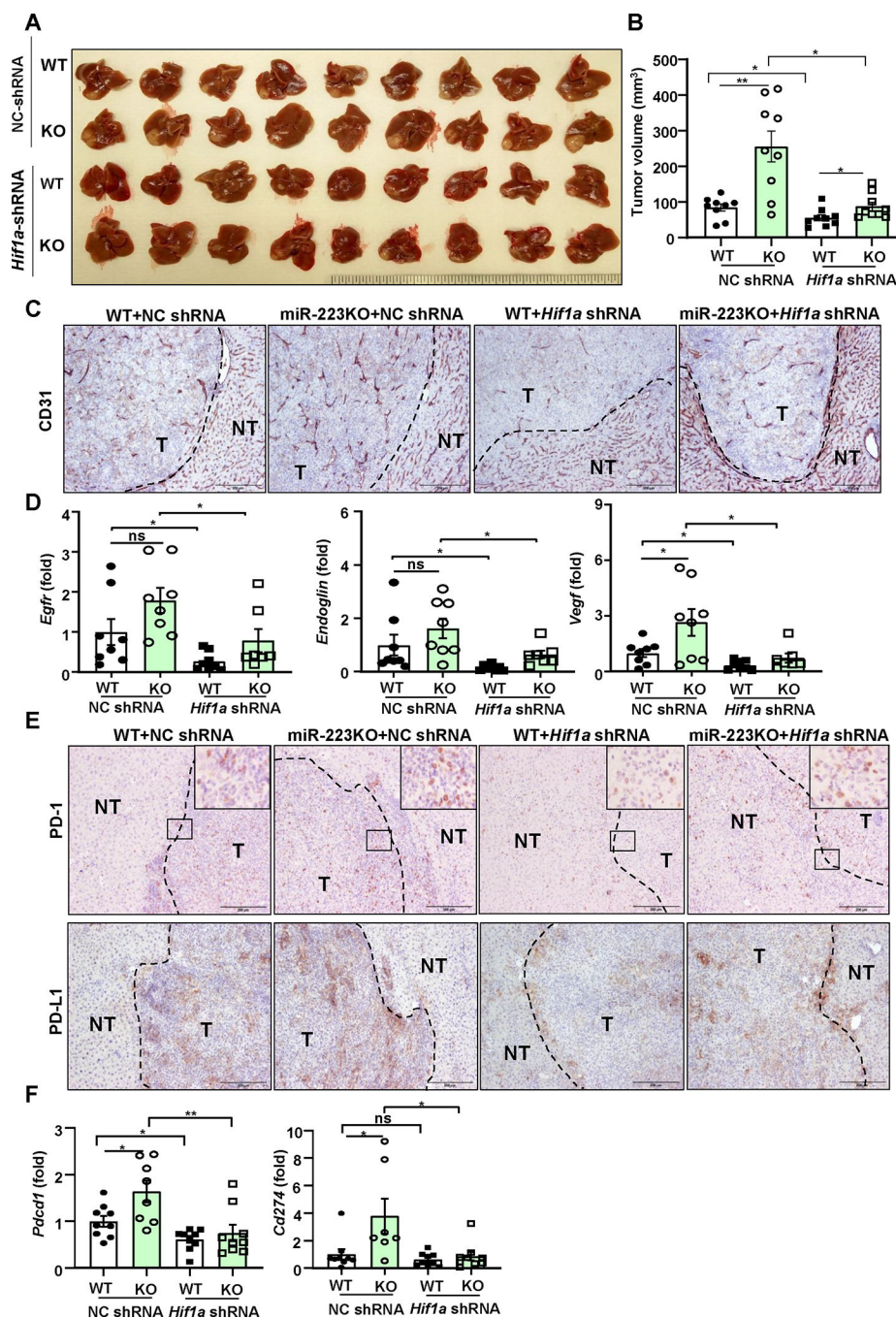


Figure 7. Knockdown of *Hif1a* in HCC abolishes miR-223 deficiency-driven angiogenesis and PD-1/PD-L1 activation.

Four groups of mice were used: NC-shRNA or *Hif1a*-shRNA-transfected HCC in WT and miR-223KO mice in CCl₄ plus Hepa1-6 orthotopic HCC model. NC-shRNA stands for negative control of *Hif1a*-shRNA. (A) Gross images of HCC tumor masses. (B) Tumor volumes were analyzed. (C) Representative images of CD31 staining in HCC sections (NT: non-tumor region; T: tumor region) of 4 groups are shown; scale bar=200 μ m. (D) RT-qPCR analyses of angiogenesis-related genes in HCC tissues. (E) Representative images of PD-1/PD-L1 staining in HCC section of 4 groups are shown. The specific enlarged regions are

shown on the right upper corner of the image. The numbers of PD-L1⁺ and PD-1⁺ cells were quantified and are shown in Supporting Figure 11E. (F) RT-qPCR analyses of *Pdcd1* and *Cd274* mRNA levels in adjacent non-tumor samples. values represent means \pm SEM. * $P < 0.05$, ** $P < 0.01$.

Author Manuscript

Author Manuscript

Author Manuscript

Author Manuscript

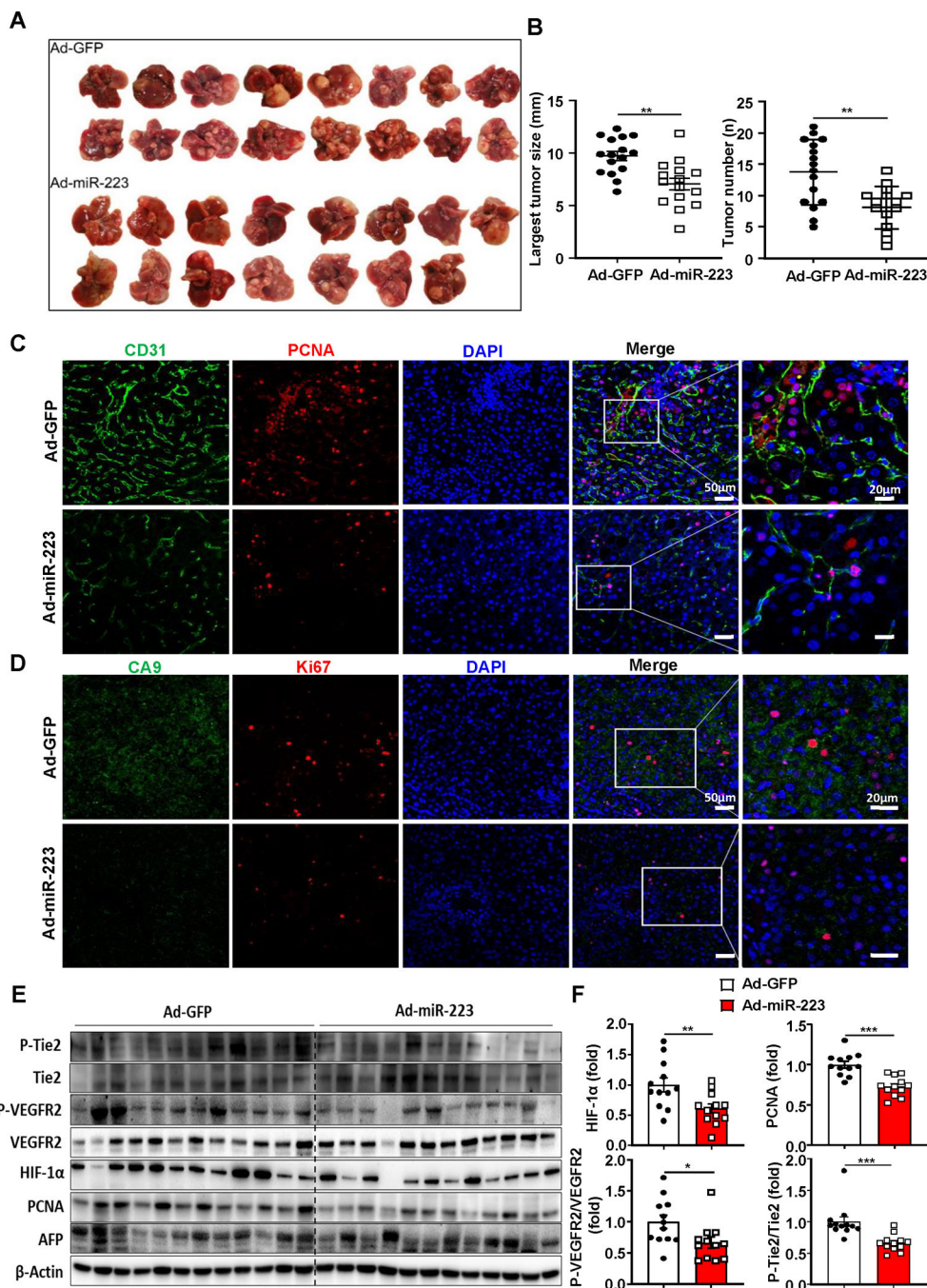


Figure 8. Administration of Ad-miR-223 attenuates PD-1/PD-L1 activation and tumor angiogenesis, hypoxia in DEN+CCl₄-induced HCC.

C57BL/6J mice were treated with DEN+CCl₄ as described in Figure 1, and were treated with Ad-miR-223 or Ad-GFP. (A) Gross images of HCC tumor masses from Ad-miR-223 and control Ad-GFP-treated mice are shown. (B) The largest tumor diameter and the number of tumor masses between Ad-GFP and Ad-miR-223-treated mice were analyzed. (C, D) Representative immunofluorescence staining of CD31/PCNA (panel C) or hypoxia marker (CA9)/proliferative marker (Ki-67) (panel D) in tumor regions of Ad-GFP and Ad-miR-223-treated liver samples are shown. Relative CD31 and CA9 intensity, the percentages of PCNA

and Ki67 positive cells were quantified and are shown in Supporting Figure 12B. (E, F) Protein levels of phosphorylated Tie-2 and VEGFR2 (p-TIE-2, p-VEGFR2), HIF-1 α , PCNA and AFP were determined and quantified by western blot. Values represent means \pm SEM. * P < 0.05, ** P < 0.01, *** P < 0.001.

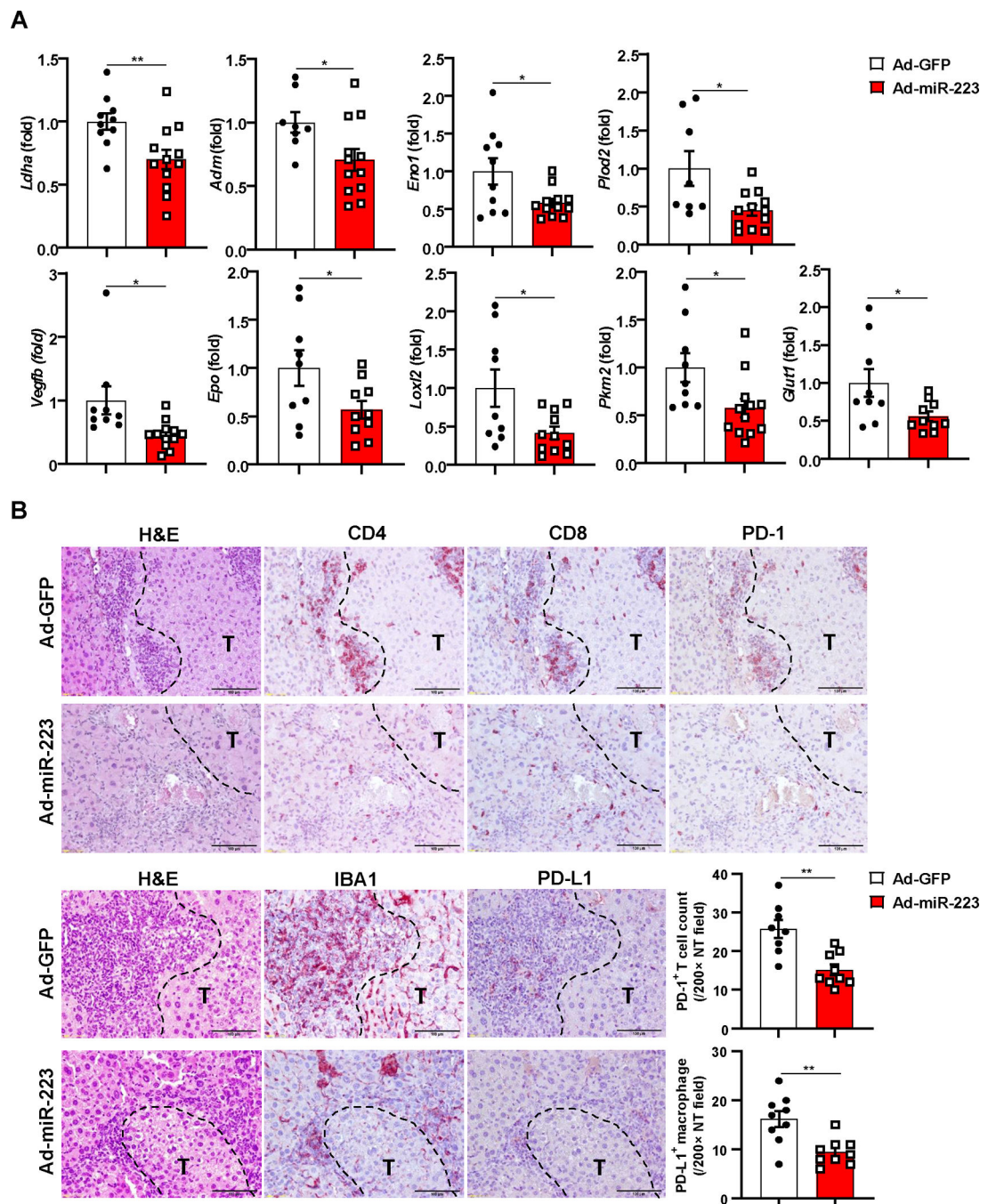


Figure 9. Overexpression of miR-223 *in vivo* reduces tumor hypoxia and PD-1/PD-L1 expression in DEN+CCl₄-induced HCC.

C57BL/6J mice were treated with DEN+CCl₄ as described in Figure 1, and were treated with Ad-miR-223 or Ad-GFP. (A) RT-qPCR analyses of HIF-1 α target genes in HCC samples from Ad-miR-223 and control Ad-GFP-treated mice. (B) Upper panel: representative immunostaining for infiltrated PD-1⁺ CD4⁺/CD8⁺ T cells surrounding tumor region are shown. Scale bar: 200 μ m. Lower left panel: representative images for PD-L1⁺ macrophages surrounding tumor region are shown. Lower right panel: counts of PD-1⁺ T cells and PD-L1⁺ macrophages in non-tumor region (NT) were quantified and are shown.

Tumor region was labeled with ‘T’; tumor border was depicted with black dash line. Values represent means \pm SEM. * $P < 0.05$, ** $P < 0.01$.

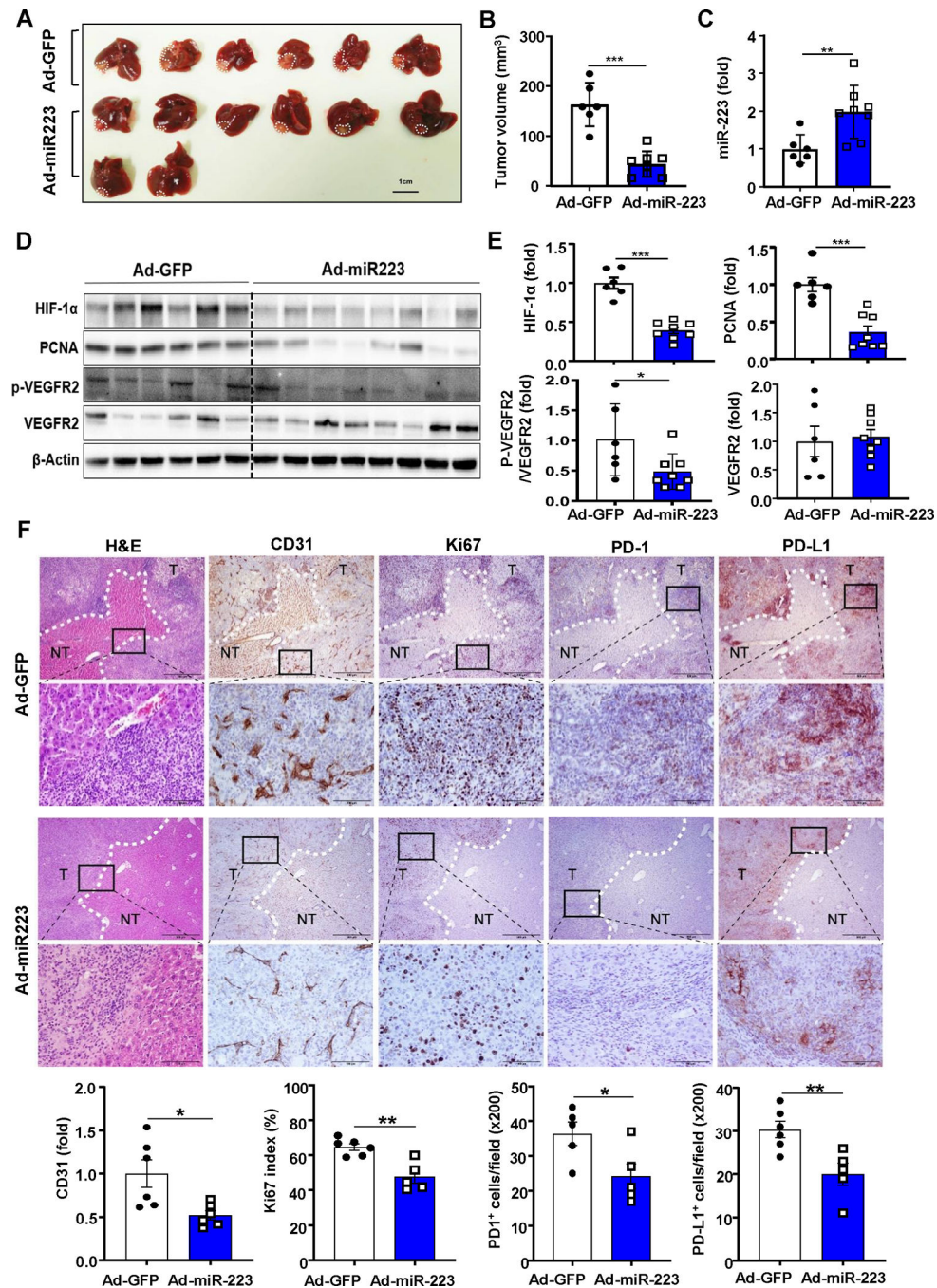


Figure 10. Administration of Ad-miR-223 suppresses PD-1/PD-L1 axis and angiogenesis in inflammation-related orthotopic HCC model.

C57BL/6J mice were treated with CCl₄ plus Hepa1-6-implantation and were treated with Ad-miR-223 (n=8) or Ad-GPF (n=6). (A) Gross images of livers. (B) Tumor volume (mm³) in Ad-GFP and Ad-miR-223 treated-mice were analyzed. (C) miR-223 levels in tumor tissues of Ad-miR-223- or Ad-GFP-treated mice were measured. (D) Protein levels of HIF-1α, PCNA, phosphorylated VEGFR2, total VEGFR2 were determined by western blot analysis. (E) Quantitative analysis of HIF-1α, PCNA, total VEGFR2 and ratio of phosphorylated VEGFR2 to total VEGFR2 (p-VEGFR2/VEGFR2 ratio). (F) Upper panel:

Representative images of H&E and immunostaining (CD31, Ki-67, PD-1, PD-L1) in consecutive liver sections from Ad-GFP and Ad-miR-223-treated groups are shown. Lower panel: quantification of CD31, Ki-67, PD-1, PD-L1 staining. Tumor region was surrounded by dashed white line. (T: tumor region). Values represent means \pm SEM. * P < 0.05, ** P < 0.01, *** P < 0.001.

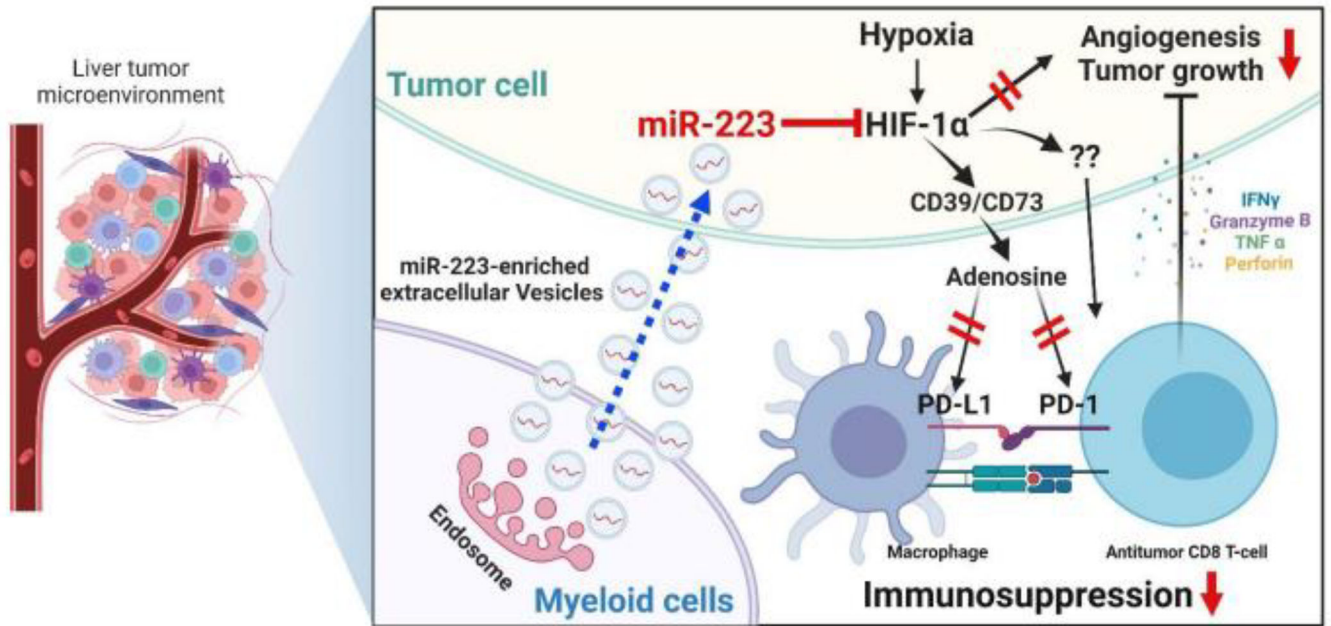


Figure 11. A model depicting the anti-HCC role of miR-223 in blocking tumor hypoxia-driven PD-1/PD-L1 immunosuppression and angiogenesis.

In chronic inflammation-associated HCC, the source of miR-223 in HCCs is likely transferred via the extracellular vesicles from myeloid cells including neutrophils and macrophages, which are enriched in adjacent tumor regions. MiR-223 directly inhibits *Hif1a*/HIF-1 α in HCC cells and subsequently alters hypoxic tumor microenvironment, thereby limiting hypoxia-driven angiogenesis and immunosuppression. HIF-1 α -mediated upregulation of CD39/CD73-adenosine pathway contributes to PD-1 and PD-L1 upregulation in immune cells, which is suppressed by miR-223.